

DIFFRACTIVE DIJET PRODUCTION AT CDF



Konstantin Goulios
(for the CDF II Collaboration)



PHYSICAL REVIEW D **86**, 032009 (2012)

DIFFRACTION 2012

International Workshop on Diffraction in High-Energy Physics



Puerto del Carmen, Lanzarote
Canary Islands (Spain)

VIK Hotel San Antonio
September 10 - 15, 2012

CONTENTS

- Introduction / motivation
- Diffractive dijets
- Summary

STUDIES OF DIFFRACTION IN QCD

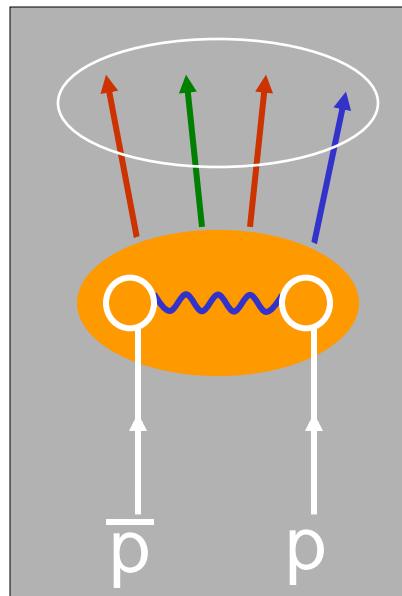
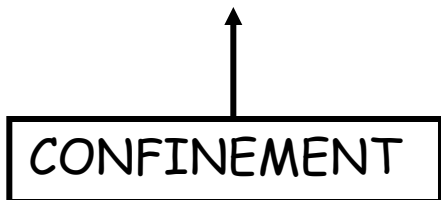
Non-diffractive

- ❖ color-exchange \rightarrow gaps exponentially suppressed

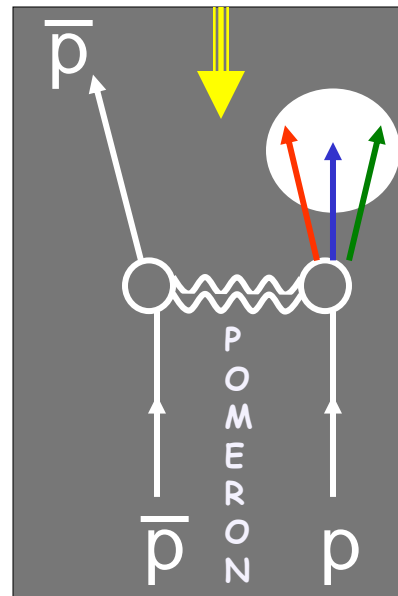
Diffractive

- ❖ Colorless vacuum exchange \rightarrow large-gap signature

Incident hadrons acquire color and break apart



rapidity gap

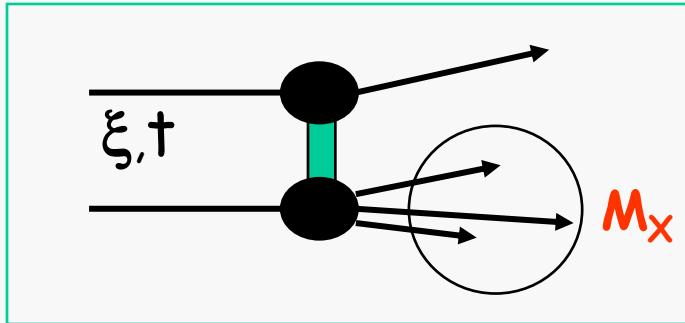


Incident hadrons retain their quantum numbers remaining colorless

Goal: probe the QCD nature of the diffractive exchange

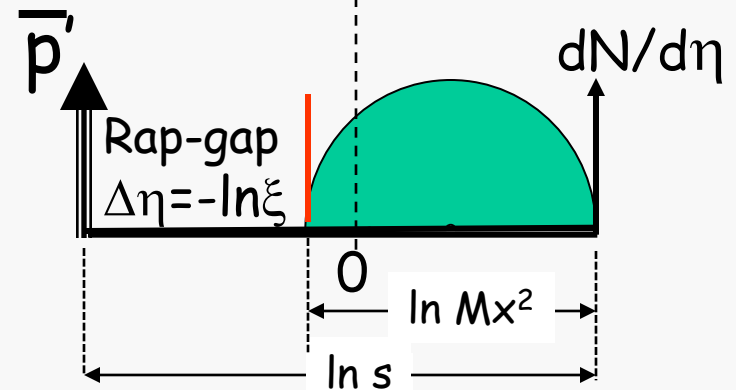
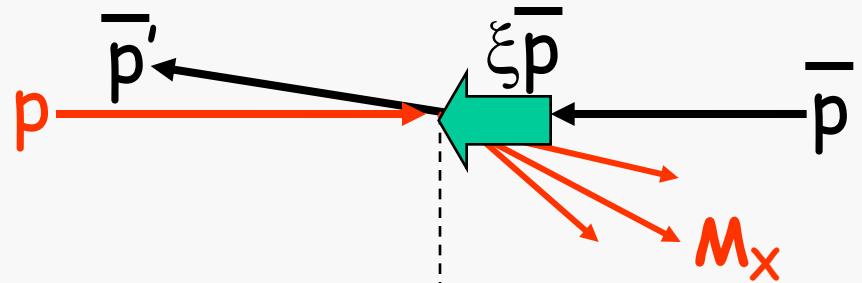
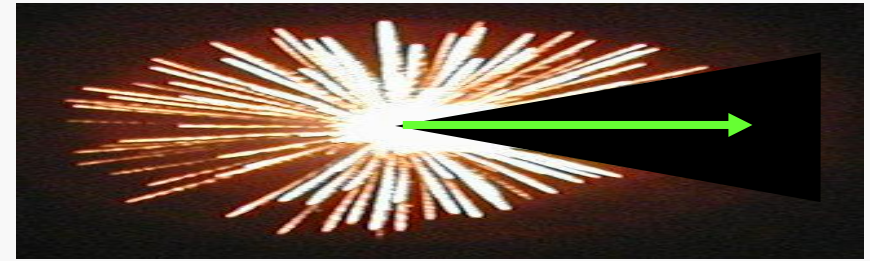
DEFINITIONS

SINGLE DIFFRACTION



$$1 - x_L \equiv \xi = \frac{M_x^2}{s}$$

$$\xi^{\text{CAL}} = \frac{\sum_{i=1}^{\text{all}} E_T^{i\text{-tower}} e^{-\eta_i}}{\sqrt{s}}$$



since no radiation \rightarrow
no price paid for increasing
diffractive gap size

$$\left(\frac{d\sigma}{d\Delta\eta} \right)_{t=0} \approx \text{constant} \Rightarrow \frac{d\sigma}{d\xi} \propto \frac{1}{\xi} \Rightarrow \frac{d\sigma}{dM^2} \propto \frac{1}{M^2}$$

DIFFRACTION AT CDF

Elastic scattering



$\sigma_T = \text{Im } f_{el}(t=0)$

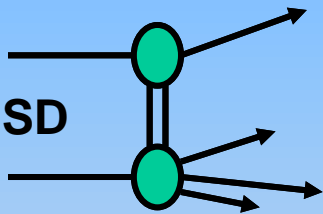


OPTICAL THEOREM

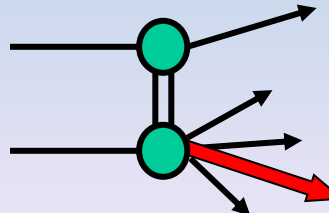
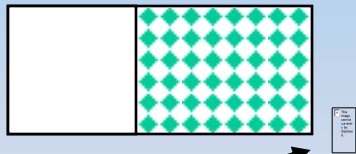
Total cross section



SD

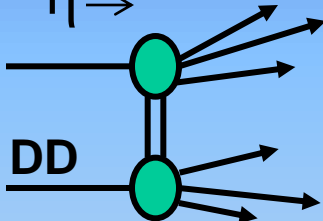


Single Diffraction or Single Dissociation



JJ, b, J/ψ, W

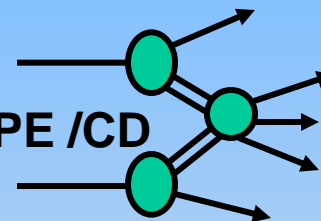
DD



Double Diffraction or Double Dissociation



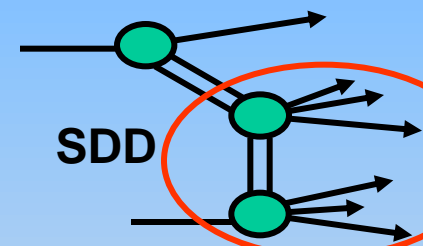
DPE /CD



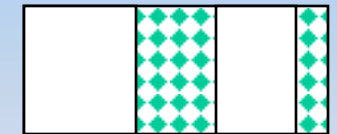
Double Pom. Exchange or Central Dissociation



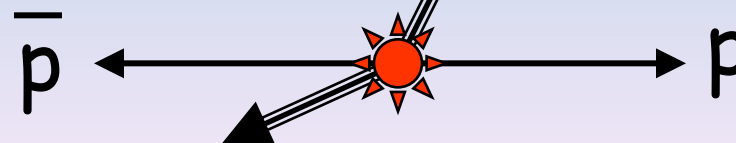
SDD



Single + Double Diffraction (SDD)

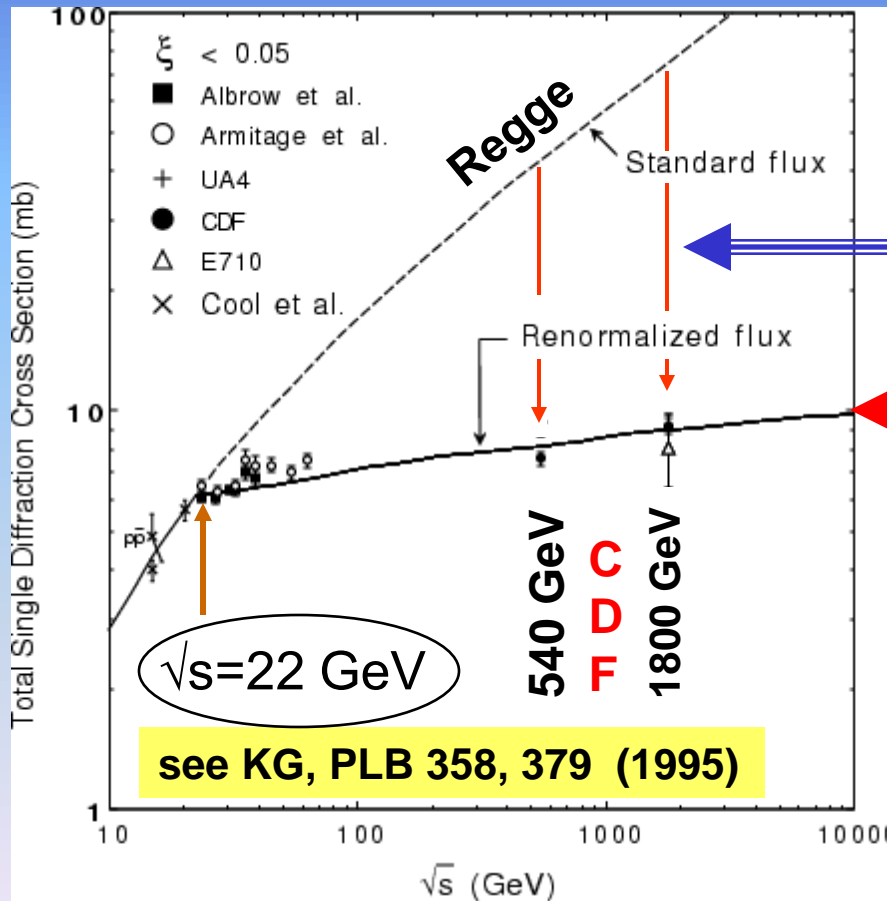
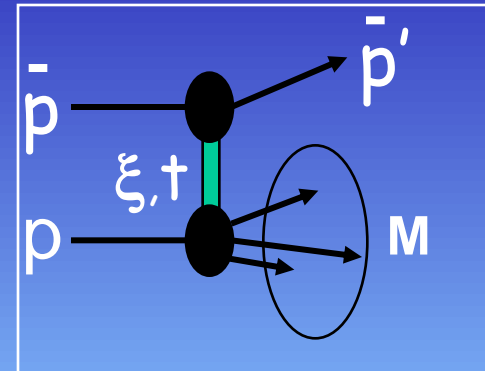


exclusive JJ...ee...μμ...γγ



FACTORIZATION BREAKING IN SOFT DIFFRACTION

→ diffractive x-section suppressed relative to Regge prediction as \sqrt{s} increases




Factor of ~ 8 (~ 5)
 suppression at
 $\sqrt{s} = 1800$ (540) GeV

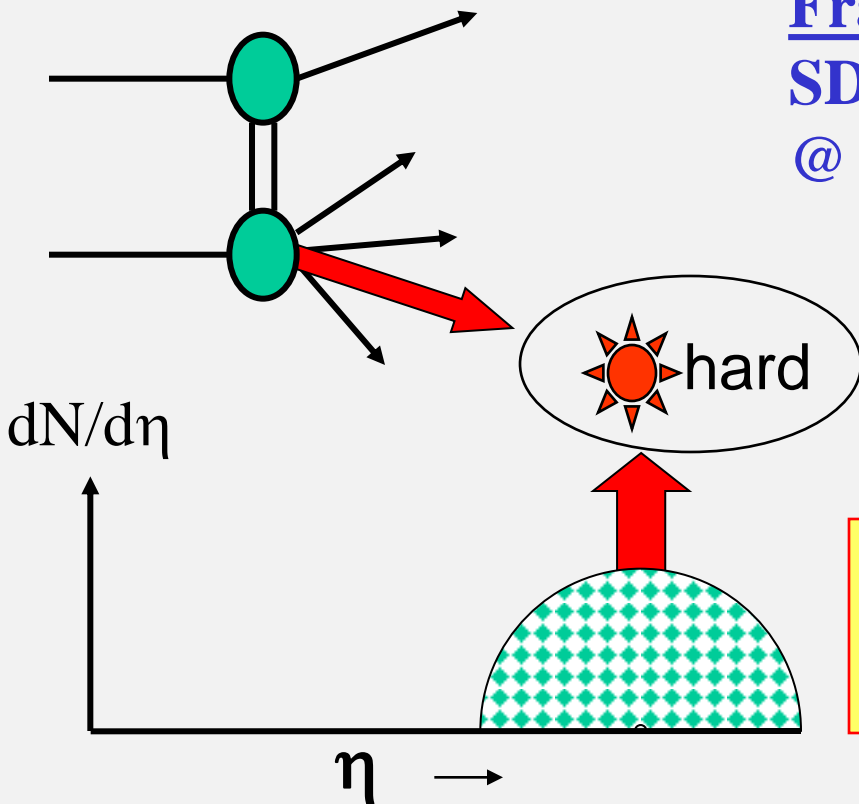
RENORMALIZATION

Question:
 does factorization breaking
 affect t -distributions?

$$\bar{p}p \rightarrow (\text{Sun} + X) + \text{gap}_p \text{ or } \text{gap}_{pbar}$$

Fraction:
SD/ND ratio
@ 1800 GeV

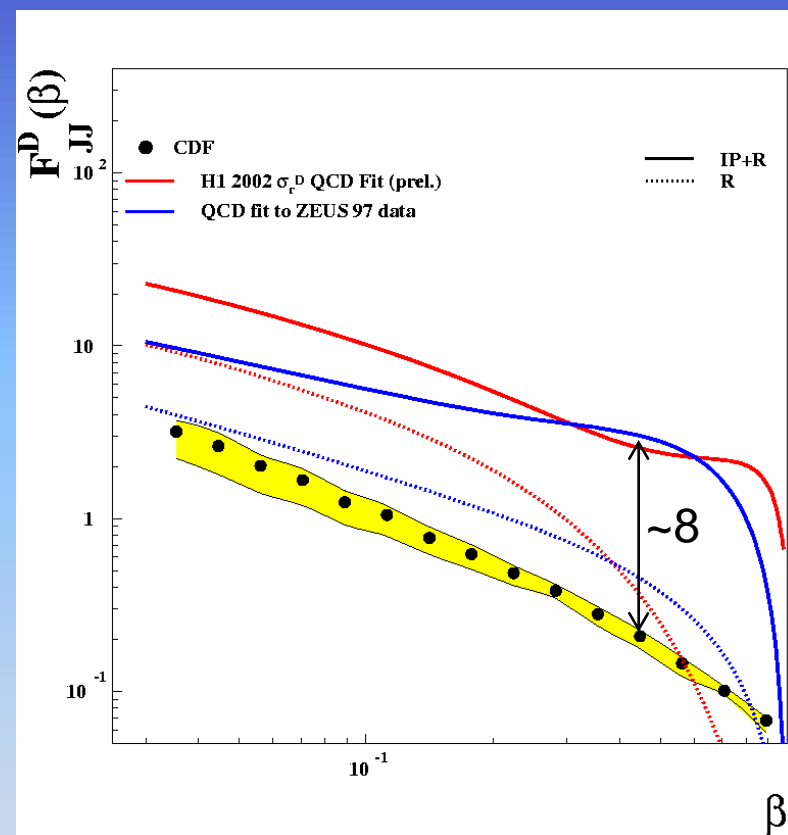
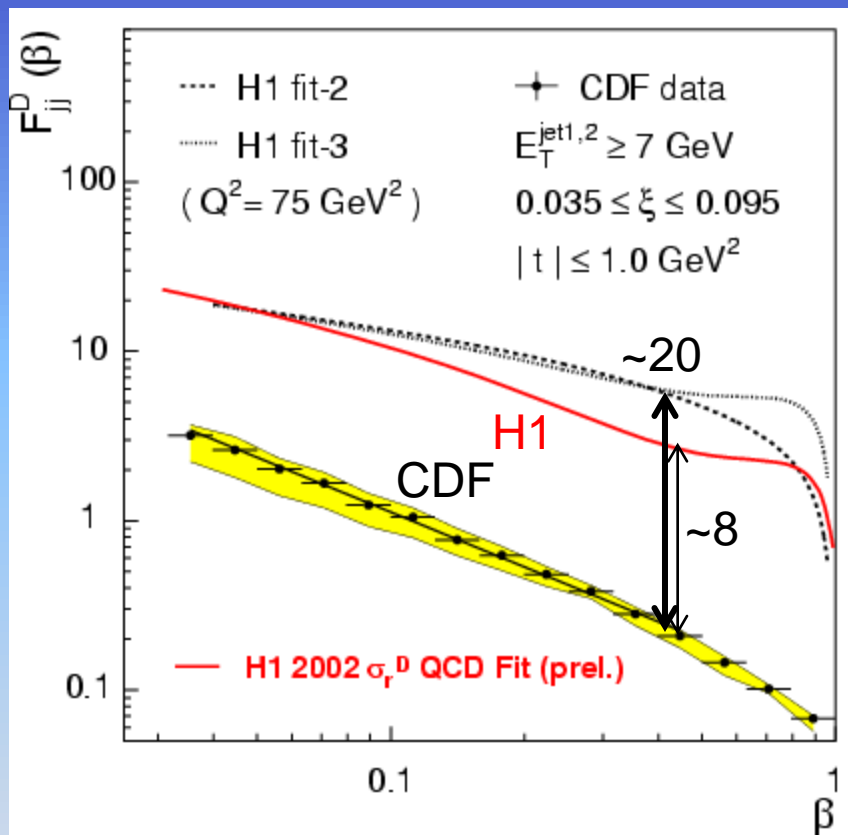
	Fraction %
JJ	0.75 +/- 0.10
W	1.15 +/- 0.55
b	0.62 +/- 0.25
J/ψ	1.45 +/- 0.25



All fractions ~ 1%
(differences due to kinematics)

➤ ~ **FACTORIZATION !**

Diffractive dijets in Run I

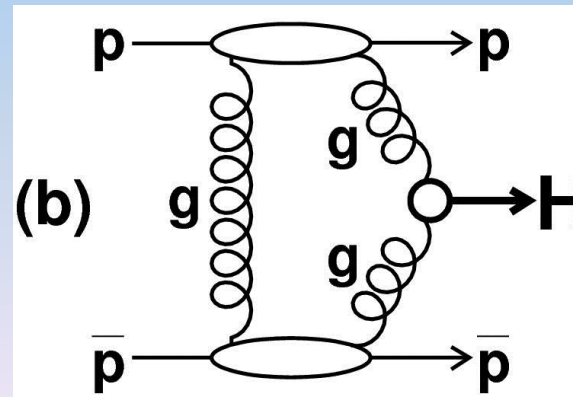
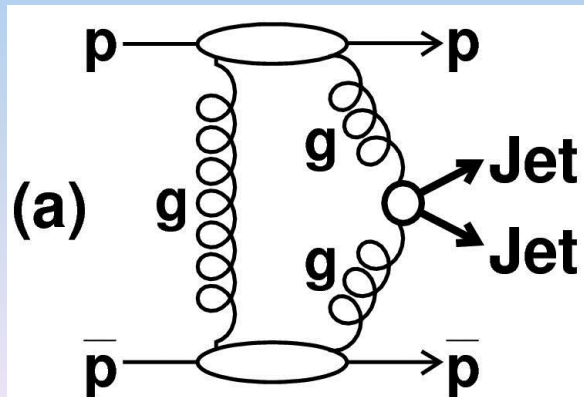
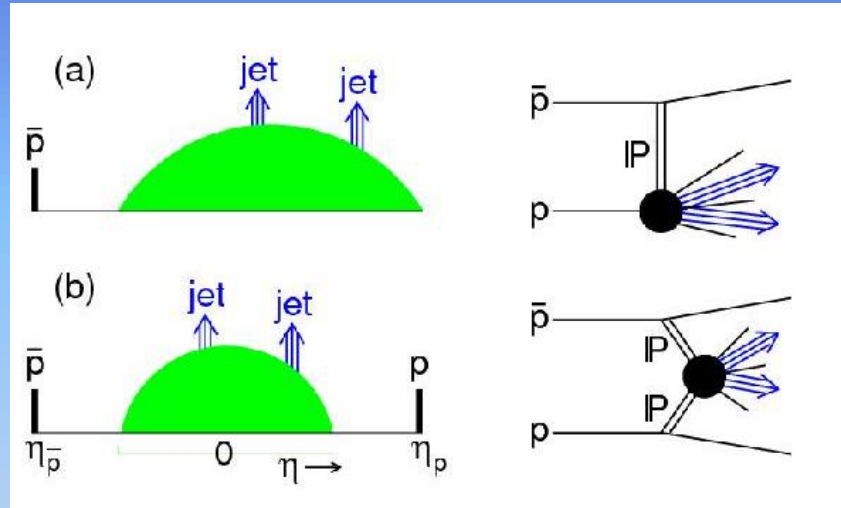


All hard-diffraction processes in Run I were found to be suppressed by a factor of ~ 8 relative to predictions based on HERA-measured PDFs.

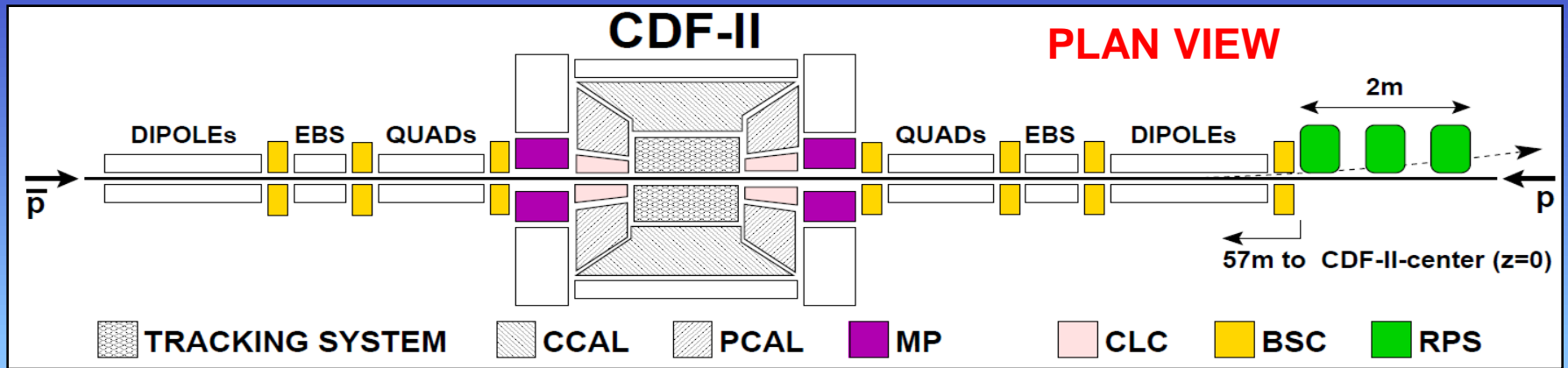
Excusive dijets

Calibrate diffractive Higgs production models

Phys. Rev. D 77, 052004 (2008)



THE CDF II DETECTOR



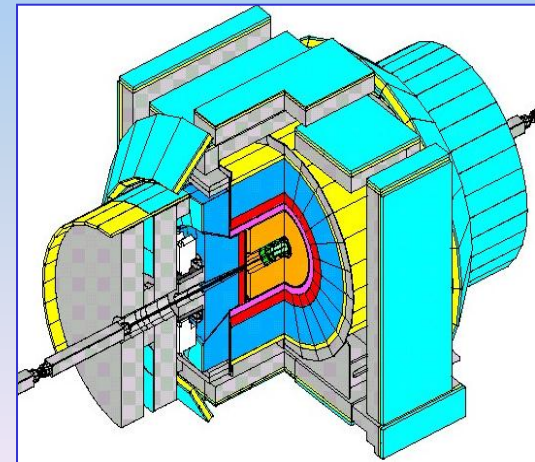
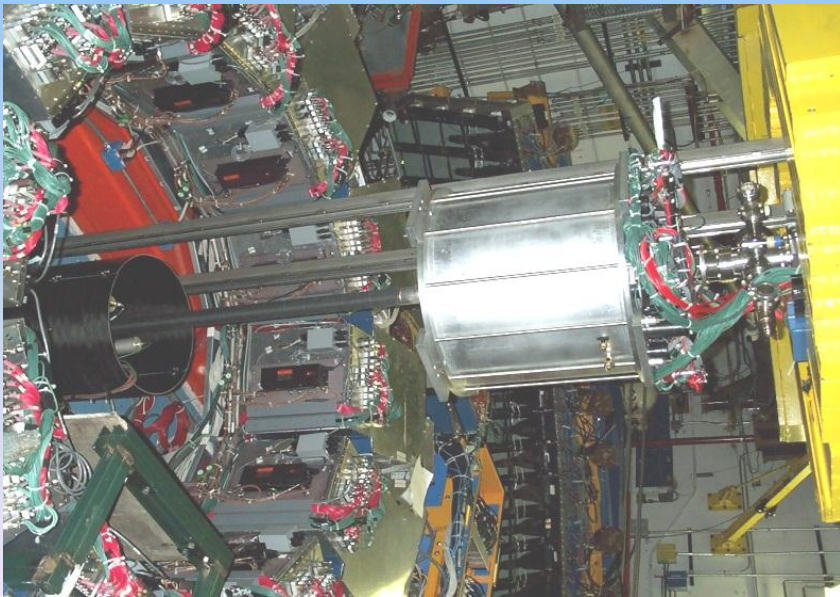
$|\eta| < 2$

$\leftarrow |\eta| < 3.6 \rightarrow$

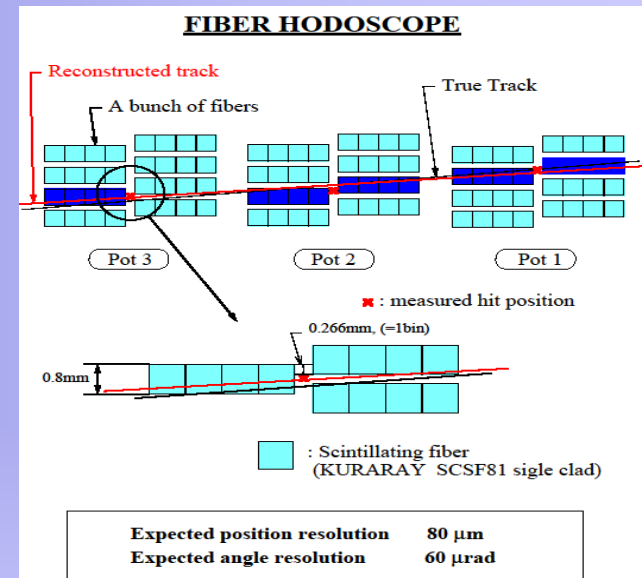
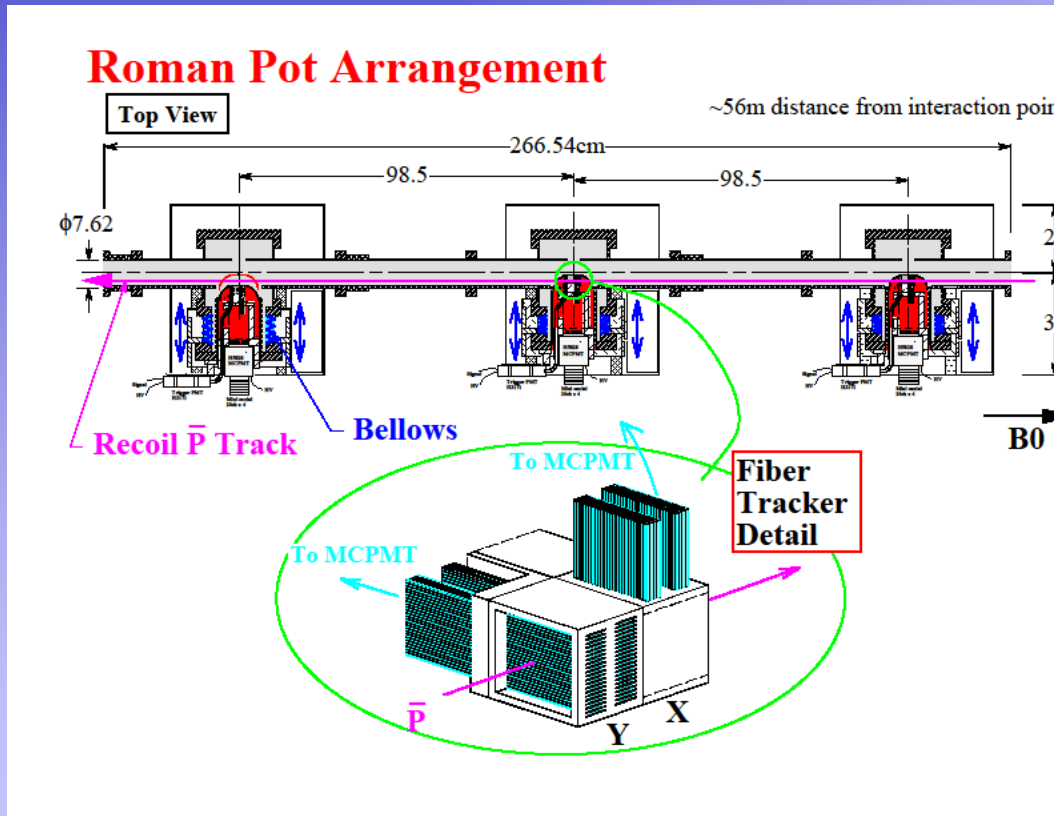
$3.5 < |\eta| < 5.1$

$5.4 < |\eta| < 7.4$

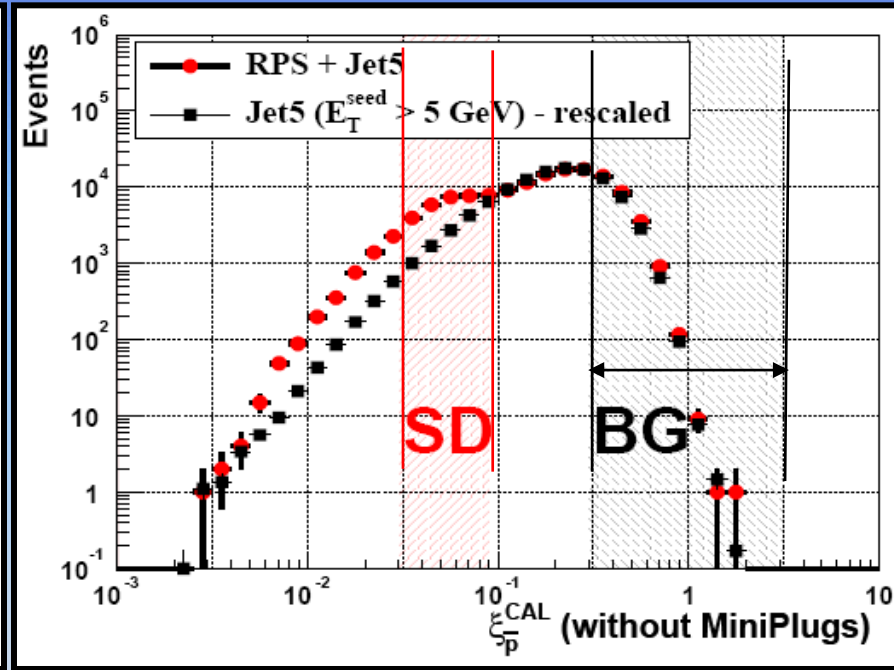
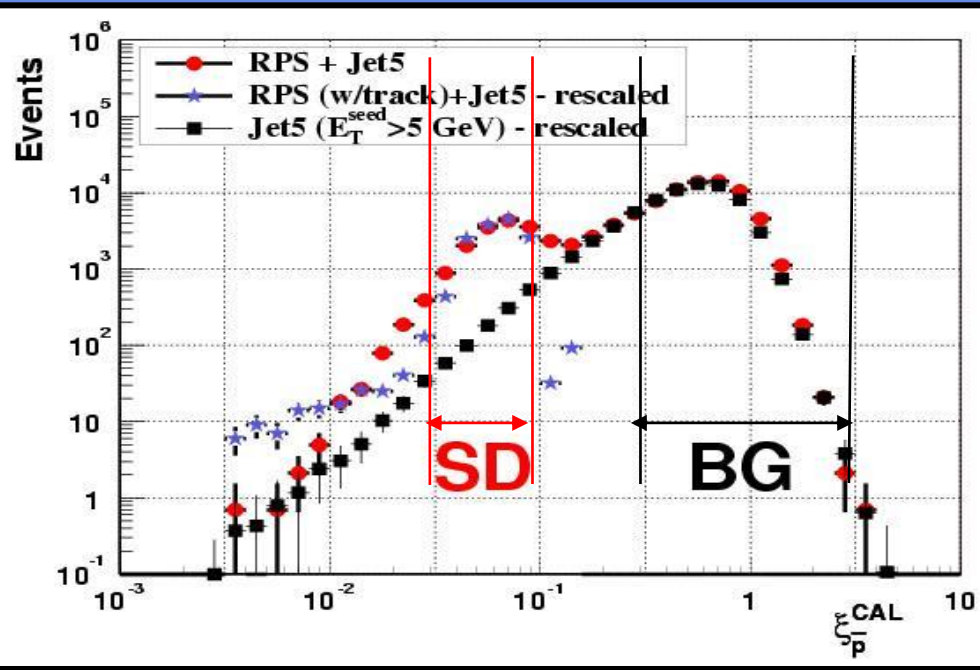
$\sim 0.03 < \xi < 0.09$ $0 < |t| < 4 \text{ GeV}^2$



The RPS



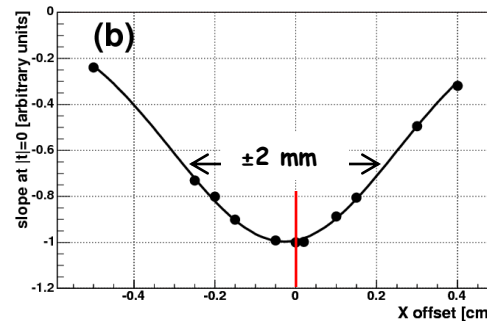
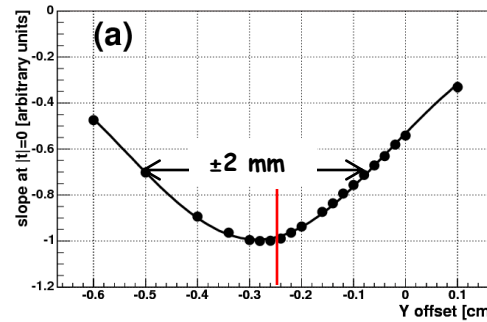
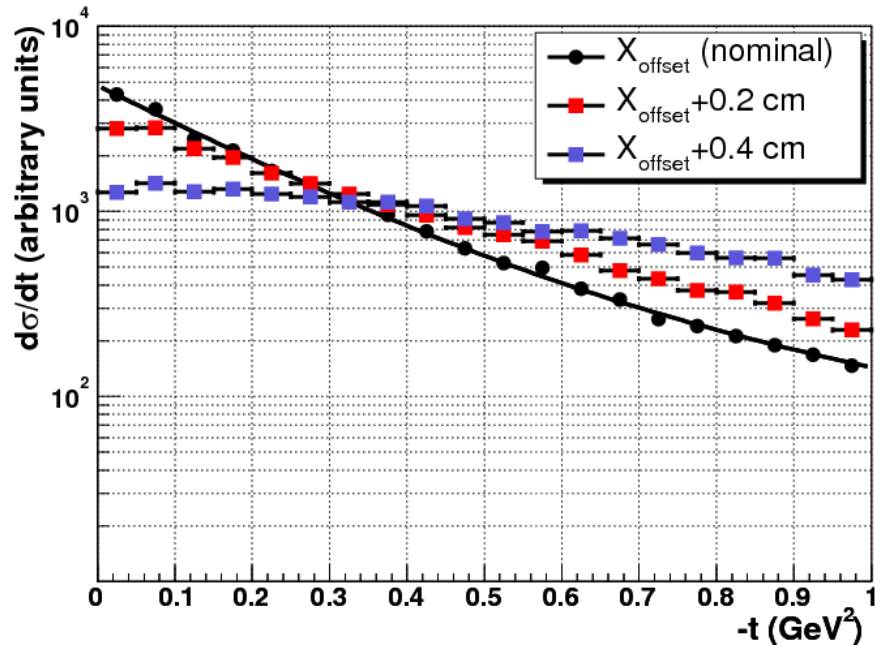
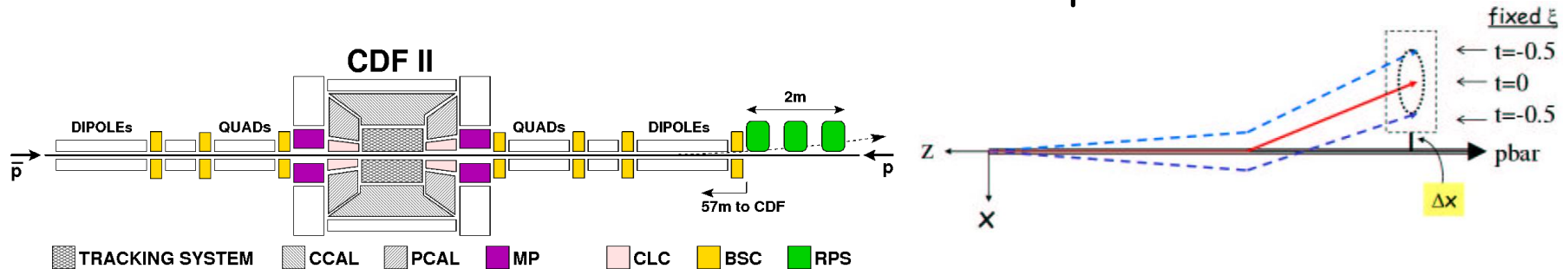
The MiniPlugs



→ overlap bgnd (BG) is reduced by including the MPs in the ξ^{CAL} evaluation

Dynamic Alignment of RPS

Method: iteratively adjust the RPS X and Y offsets from the nominal beam axis until a maximum in the b-slope is obtained @ $t=0$.

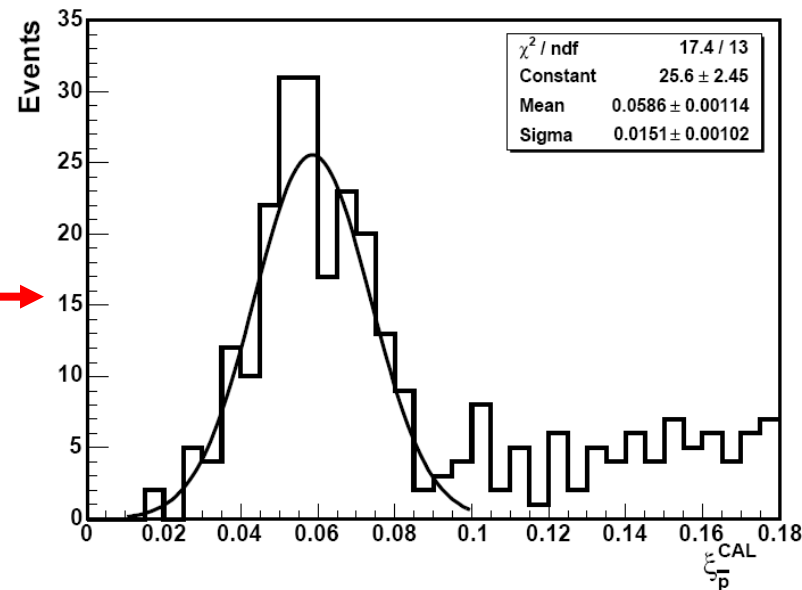
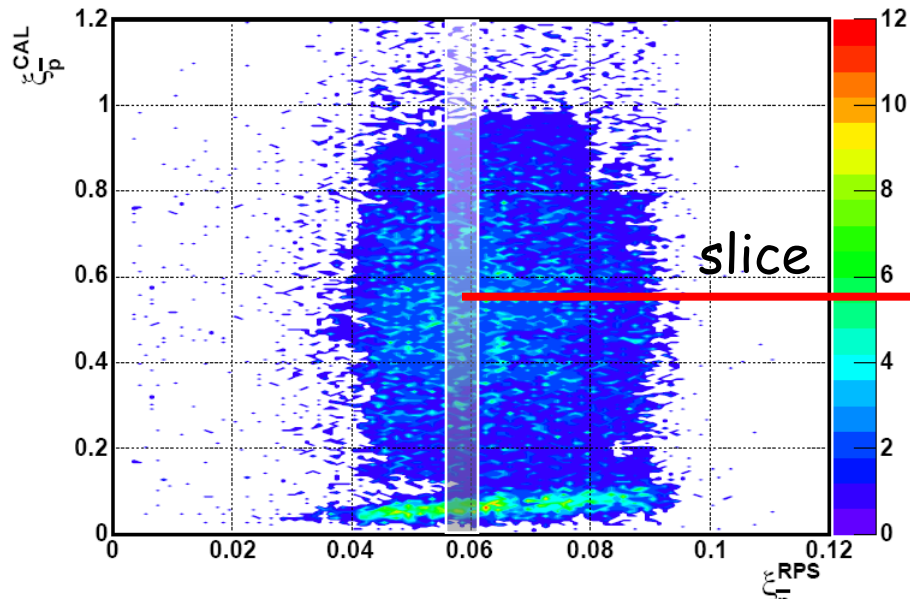


Limiting factors

- 1-statistics
- 2-beam size
- 3-beam jitter

use **RPStrk** data
width $\sim 2 \text{ mm}/\sqrt{N}$
 $N \sim 1 \text{ K events}$
 $\Delta X, \Delta Y = \pm 60 \mu$

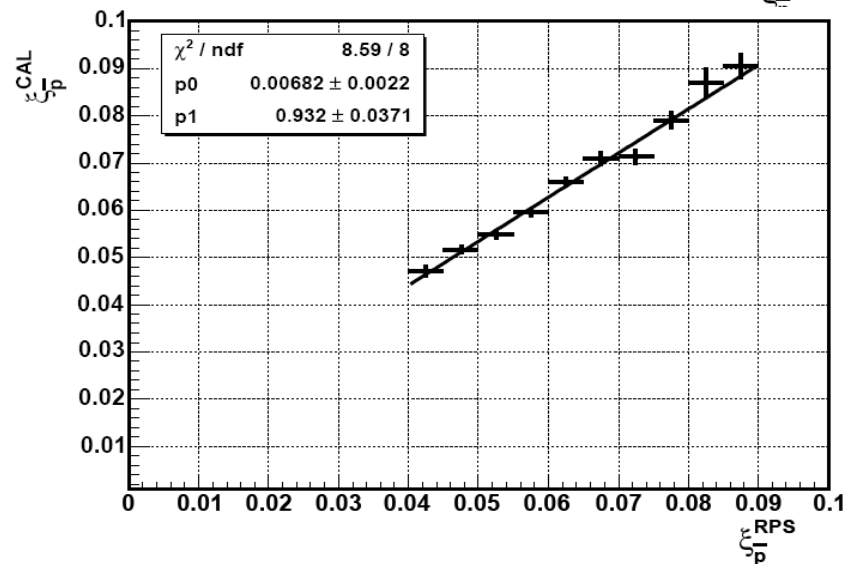
$\xi_{\bar{p}}^{\text{CAL}}$ vs $\xi_{\bar{p}}^{\text{RPS}}$



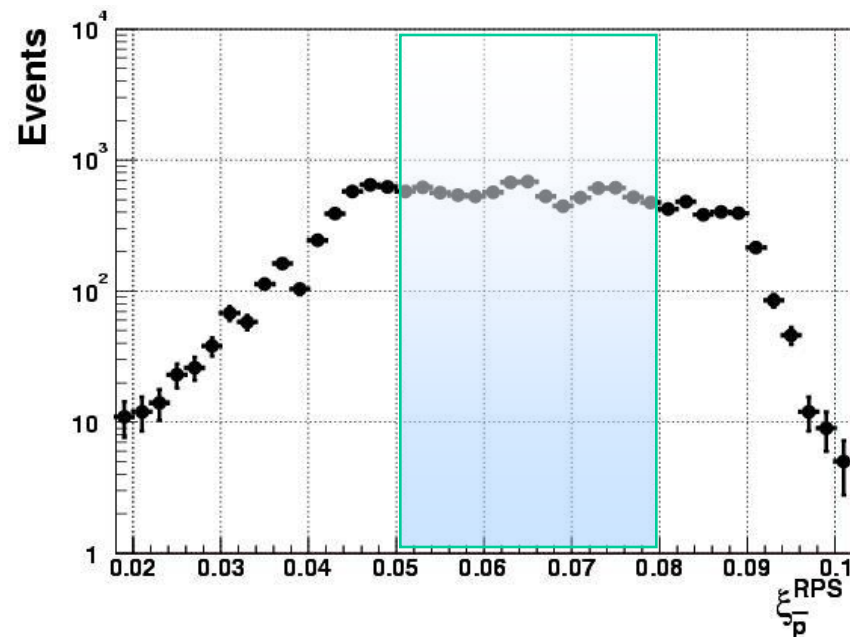
$$0.04 < \xi_{\bar{p}}^{\text{RPS}} < 0.09$$

$$\xi_{\bar{p}}^{\text{CAL}} = p^0 + p1 \cdot \xi_{\bar{p}}^{\text{RPS}}$$

$$p^0 = 0.007 \pm 0.002 \text{ and } p1 = 0.97 \pm 0.04$$



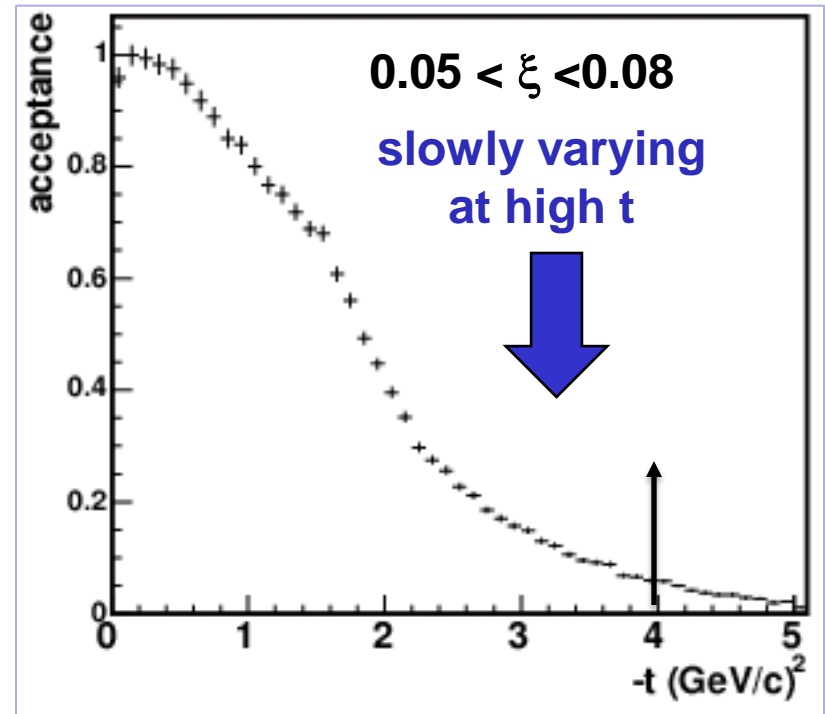
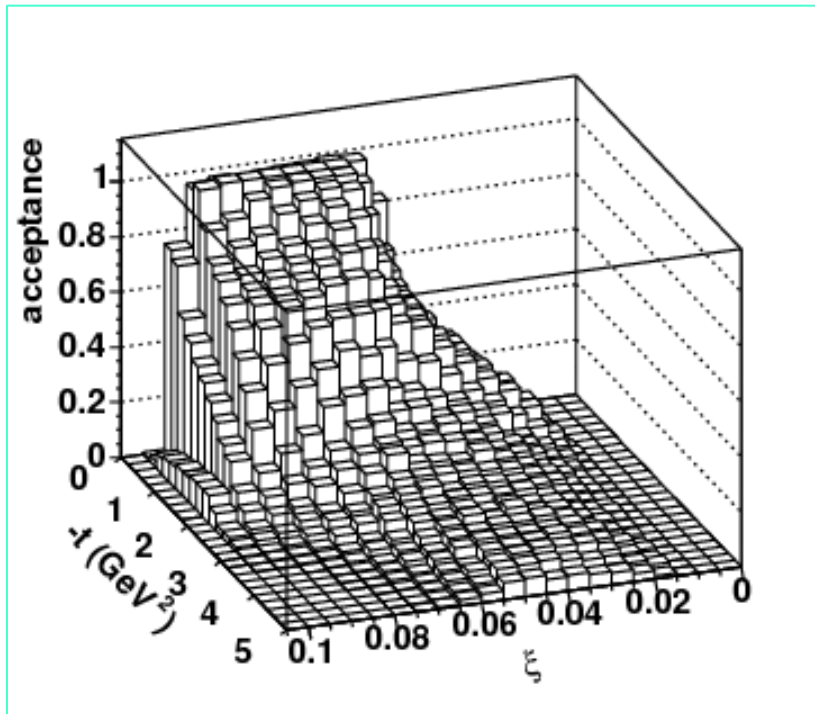
Why select $0.05 < \xi_{pbar} < 0.08$?



- be on the plateau of the $ds/d\ln\xi$ distribution
- allow enough room to avoid edge-effects
- accept enough events for good statistics

□ estimated width resulting from the $\Delta\xi$: $\Delta\tau \approx 0.47$

RPS ACCEPTANCE

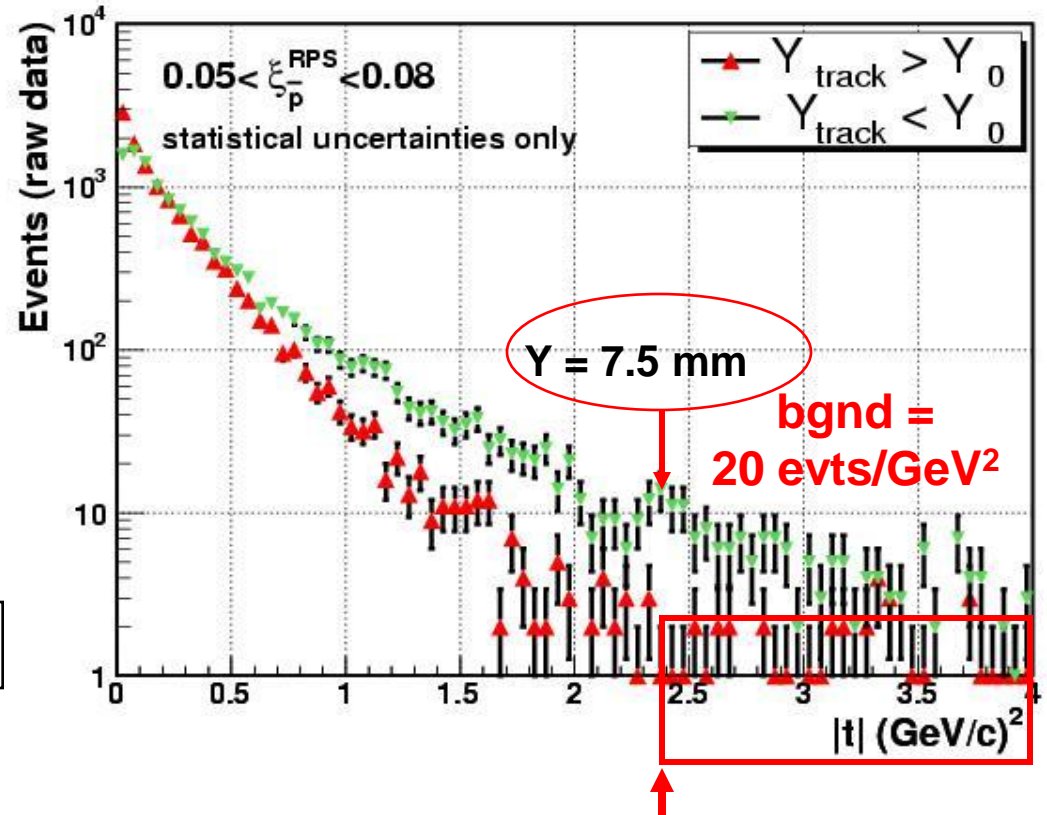
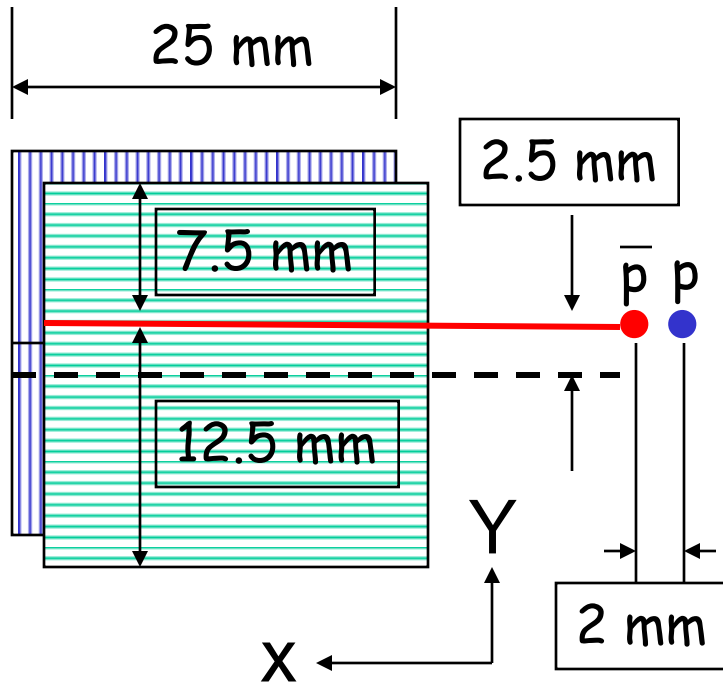


- ❑ Measure up to $-t = 4$ GeV²
- ❑ Having acceptance beyond 4 GeV² minimizes edge effects

$t > 1 \text{ GeV}^2$: asymmetric t -distributions as a tool for evaluating bgd at high t

schematic view of fiber tracker

t -distributions



- tracker's upper edge: $|t|=2.3 \text{ GeV}^2$, estimated from $t \sim \theta^2$
- the lower edge is at $|t|=6.5 \text{ GeV}^2$ (not shown)
- background level: region of $Y_{\text{track}} > Y_0$ data for $|t| > 2.3 \text{ GeV}^2$

Diffraction dijet results

<http://arxiv.org/abs/1206.3955>

PHYSICAL REVIEW D **86**, 032009 (2012)

Measurement of F_{jj}^{SD}

$$\frac{d^5\sigma_{jj}^{\text{SD}}}{dx_{\bar{p}}dx_p d\hat{t}d\xi dt} = \frac{F_{jj}^{\text{SD}}(x_{\bar{p}}, Q^2, \xi, t)}{x_{\bar{p}}} \cdot \frac{F_{jj}^{\text{incl}}(x_p, Q^2)}{x_p} \cdot \frac{d\hat{\sigma}_{jj}}{d\hat{t}}$$

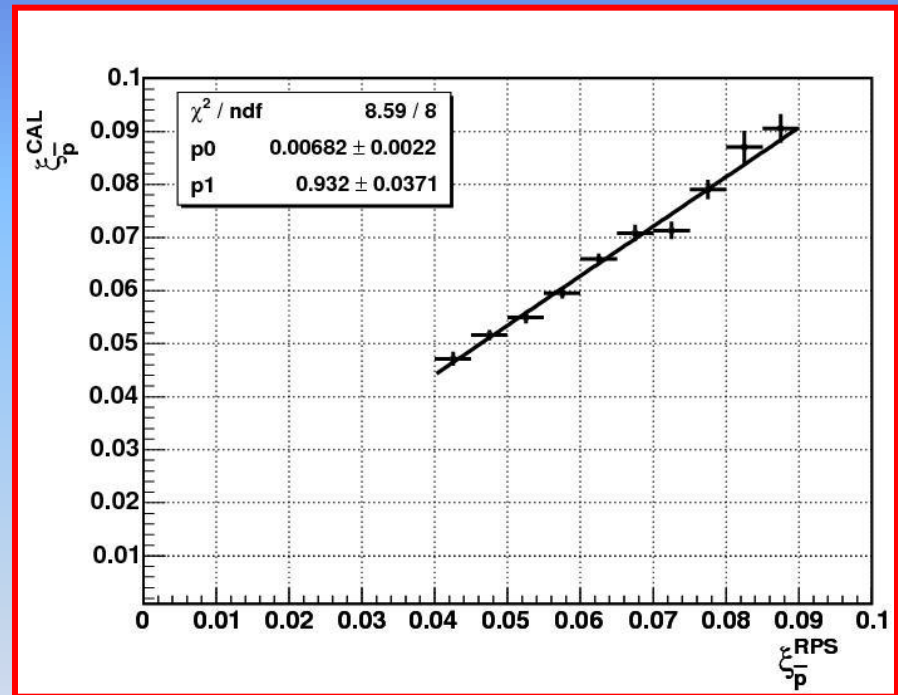
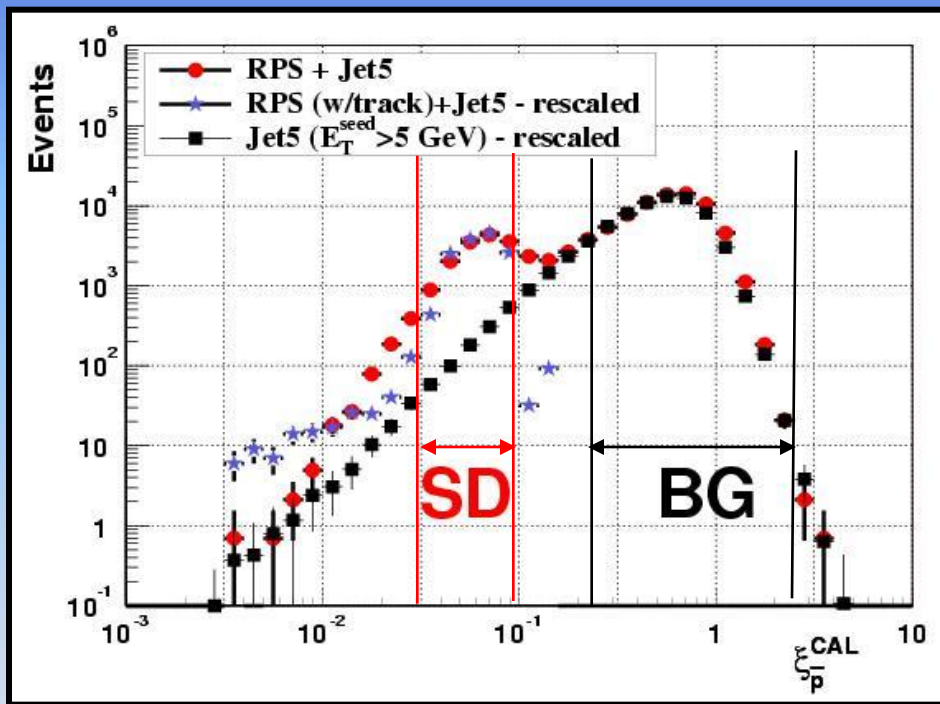
$$F_{jj}^{\text{incl}}(x, Q^2) = x \left[g(x, Q^2) + \frac{4}{9} \sum_i q_i(x, Q^2) \right]$$

$$R_{\text{SD/ND}}(x, Q^2, \xi, t) = \frac{n_{jj}^{\text{SD}}(x, Q^2, \xi, t)}{n_{jj}^{\text{ND}}(x, Q^2)} \approx \frac{F_{jj}^{\text{SD}}(x, Q^2, \xi, t)}{F_{jj}^{\text{ND}}(x, Q^2)}$$

$$F_{jj}^{\text{SD}}(x, Q^2, \xi, t) = R_{\text{SD/ND}}(x, \xi, t) \times F_{jj}^{\text{ND}}(x, Q^2)$$

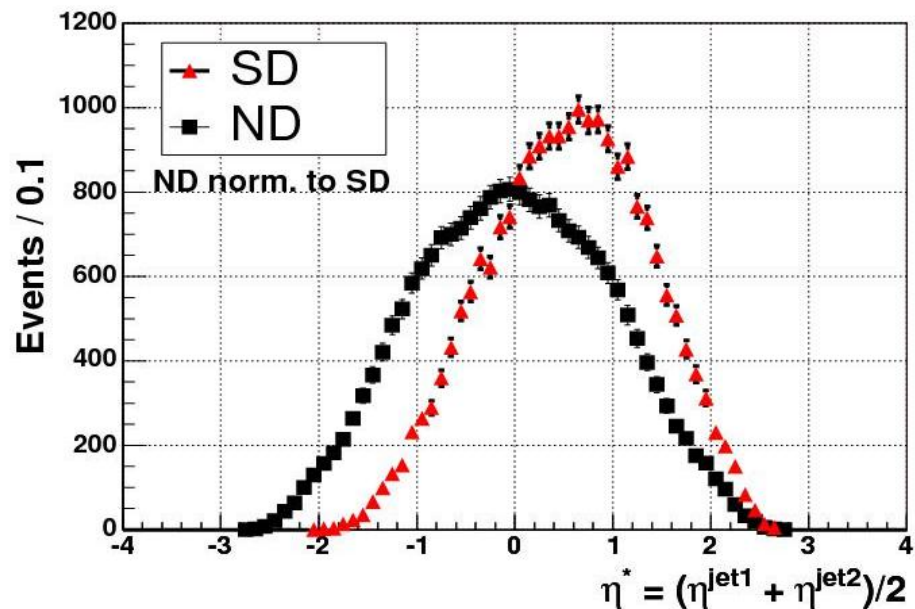
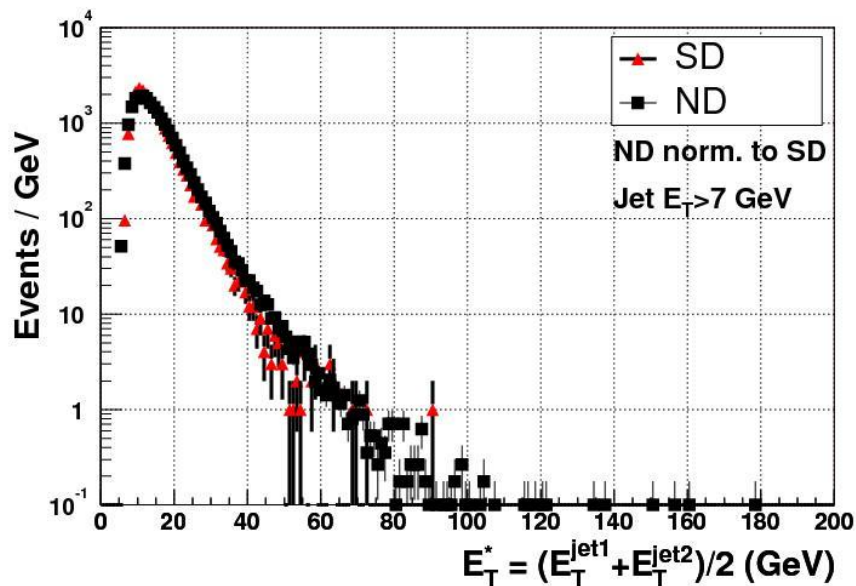
ξ^{CAL} VS ξ^{RPS}

- As RPS tracking was not available for all analyzed data, we used ξ^{CAL} and calibrated it vs ξ^{RPS} from data in which RPS tracking was available.



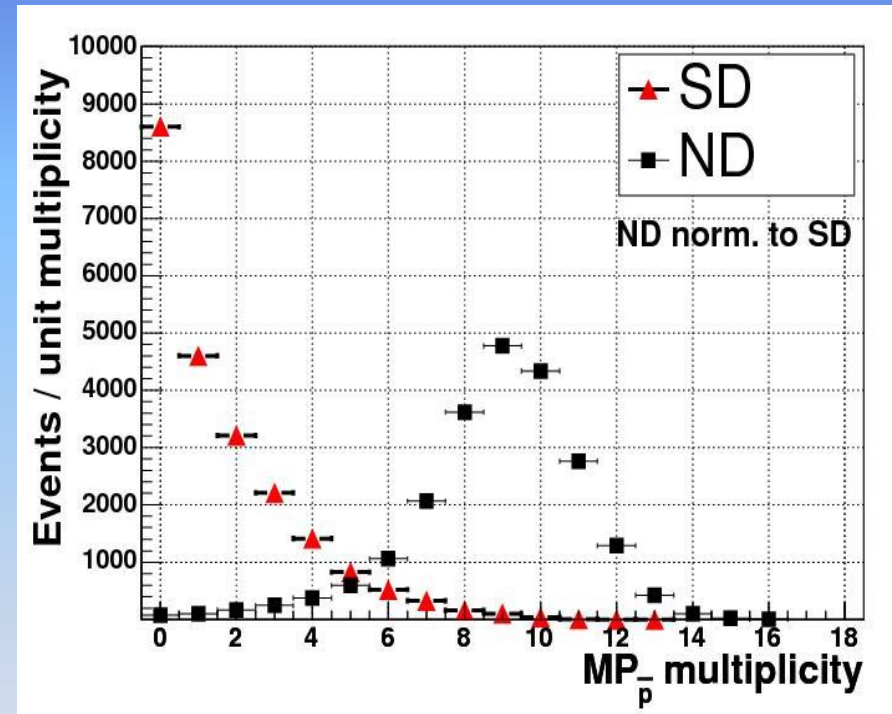
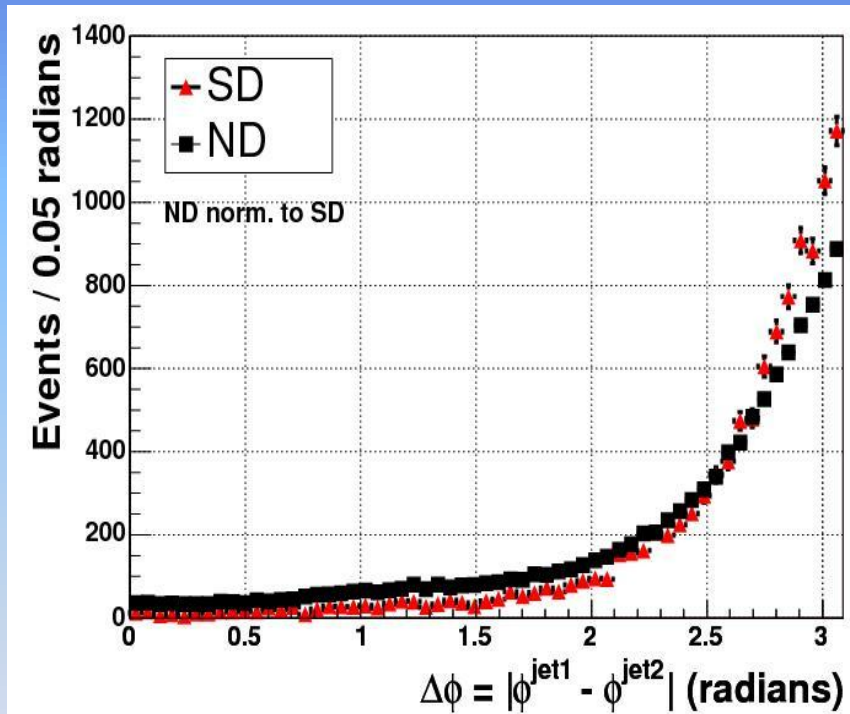
- A linear relationship is observed between ξ^{CAL} vs ξ^{RPS} in the region of ξ^{CAL} of the measurement

Average E_T^{jet} and η^{Jet}



- The SD and ND E_T^{Jet} distributions are nearly identical
- The SD η^* distribution is shifted towards the c.m.s of the Pomeron-proton collision

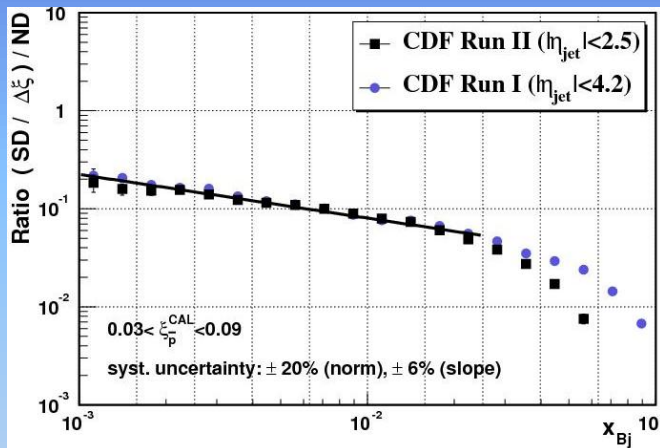
Azimuthal angle difference of jets



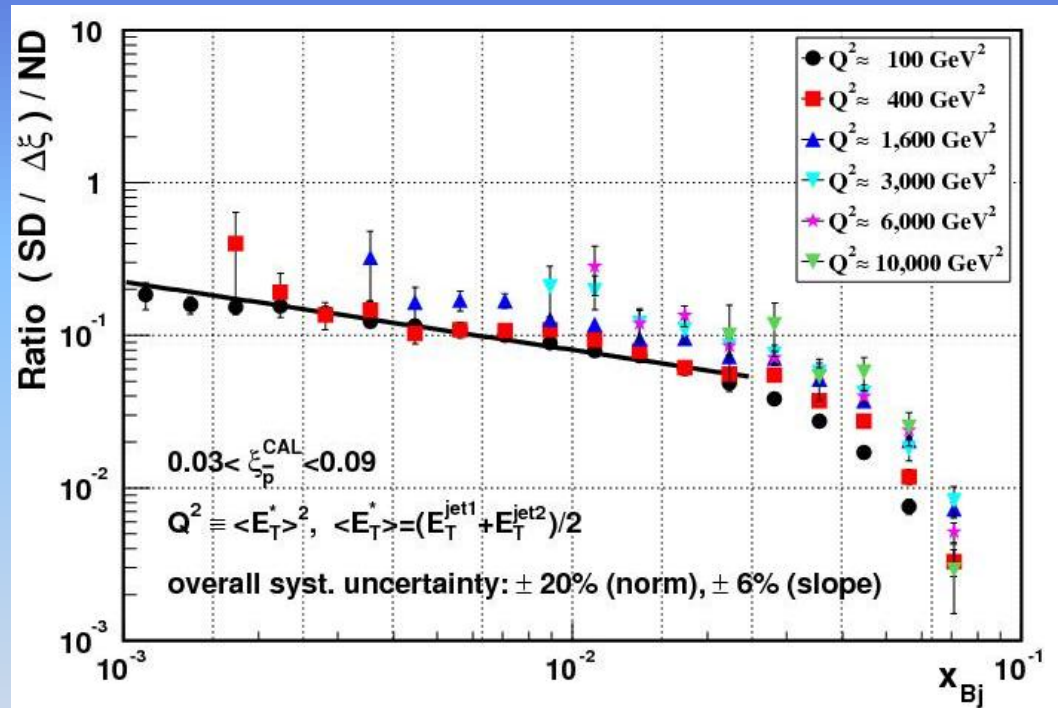
- Left: the SD distributions are more back-to-back
- Right: the SD multiplicity is peaked at zero, while the ND is peaked at 9.

x_{Bj} Distributions vs $\langle Q^2 \rangle$

$\langle Q^2 \rangle = 100 \text{ GeV}^2$



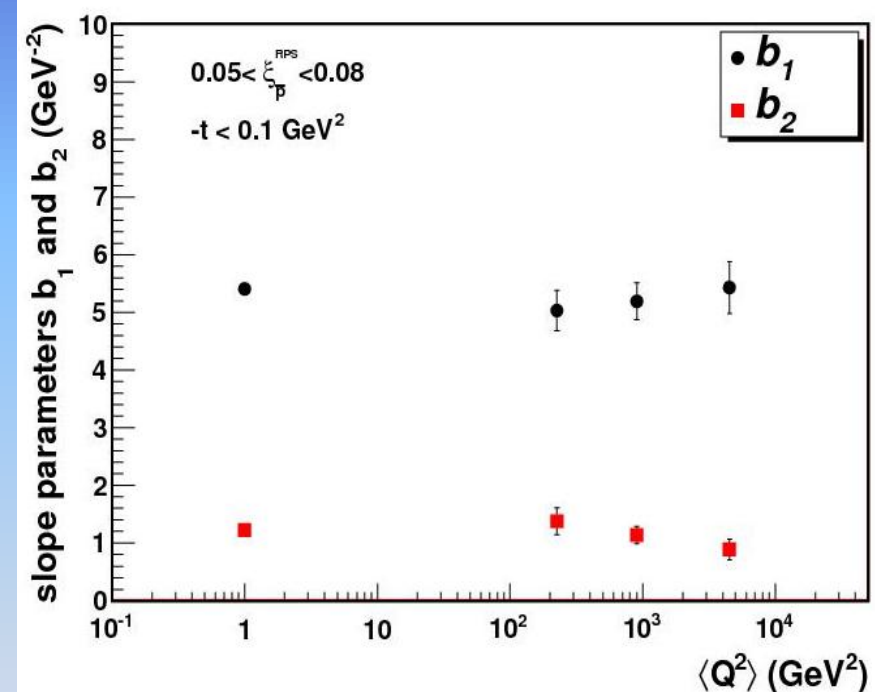
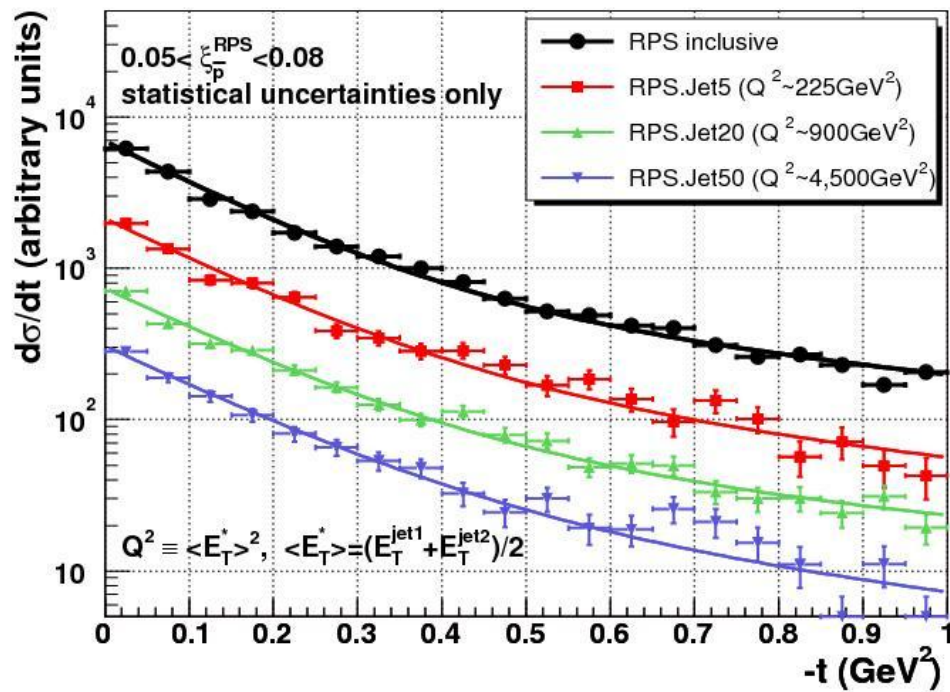
- The Run I result is confirmed.
- The drop-off on the rhs is due to the different range of the calorimeters in Run I and Run II.



□ The Bjorken- x distributions vary by only a factor of ~ 2 over a range of $\langle Q^2 \rangle$ of 2 orders of magnitude!

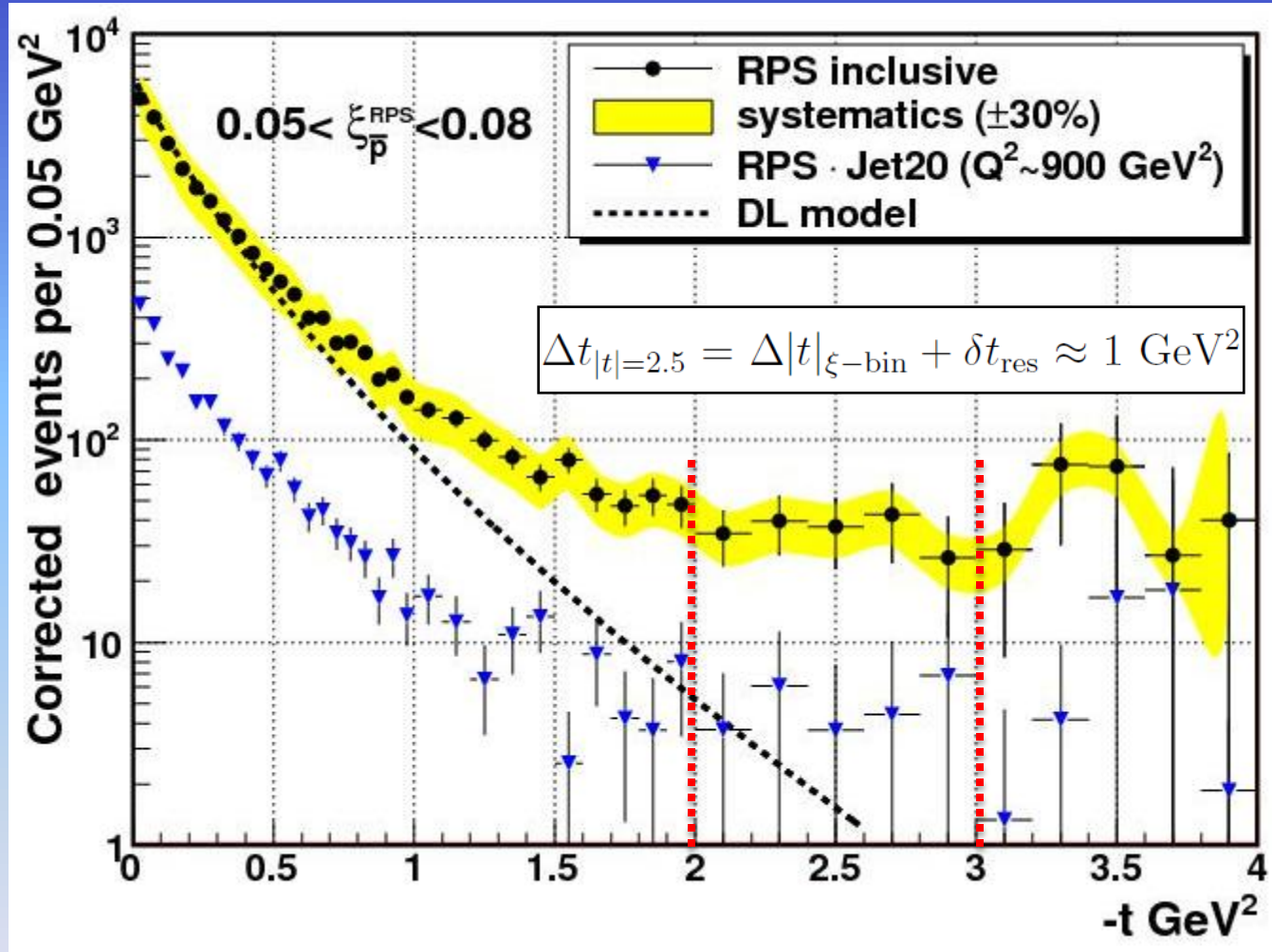
t -Distributions and Slopes vs $\langle Q^2 \rangle$ for $-t < 1 \text{ GeV}^2$

$$\frac{d\sigma}{dt} = N_{norm} (A_1 e^{b_1 t} + A_2 e^{b_2 t})$$



□ The slopes are nearly constant over a range of 4 orders of magnitude in $\langle Q^2 \rangle$!

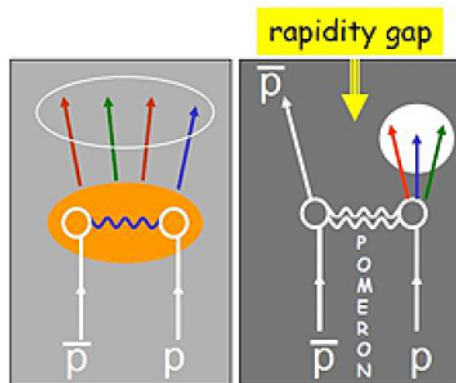
t -Distributions for $-t < 4 \text{ GeV}^2$



- The rather flat $-t$ distributions at large $-t$ are compatible with the existence of an underlying diffraction minimum around $-t \sim 2.5 \text{ GeV}^2$.

Result of the Week

Pomeron creates jets at the Tevatron



Antiproton-proton scattering by the strong interactions can be non-diffractive (left) or diffractive (right). Both original particles, the proton and antiproton, are colorless.

At the Fermilab Tevatron, protons and antiprotons were brought into collision at very high energies, equivalent to about 2,000 proton masses according to Einstein's equation, $E=mc^2$. In each collision, about 100 particles of different types are produced.

A small group at CDF has been studying what scientists call the [diffractive](#) production of jets, in which "ghost" particles help create these sprays of highly collimated particles. Exactly how are they produced?

The proton and antiproton each consists of three quarks bound by the strong force. Though the proton and antiproton are free to move inside a "bag" full of gluons and quarks, the gluons and quarks themselves are confined to each other in order to maintain something called color-neutrality.

Diffractive collisions, in the simplest case, are characterized by an outgoing antiproton, a region in which there are no particles (called a rapidity gap) and a particle cluster corresponding to the initial proton. The particle cluster is shown as the white circle in the top figure.

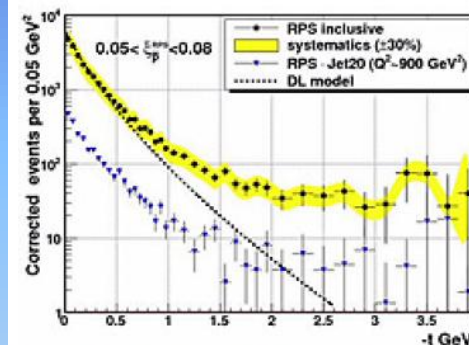
This kind of collision can be explained by the color-neutral exchange of a particle called a [pomeron](#). With its vacuum-like properties, a pomeron can escape invisibly out of the quark-gluon bag like a ghost, strike the passing proton and give it an energy injection by allowing itself to be absorbed by the proton. The energy is used to create jets that faithfully obey the equation $E=mc^2$.

The results of this experiment can be explained by a model (called DL in the figure below) at low-momentum transfers (t) between the incoming and outgoing antiproton by way of the escaping pomeron. However, the model does not explain the result for high-momentum transfers, where the data is constant. It will be interesting to see how the theory can be adapted to the high-momentum data.

These measurements are being repeated at the higher energies of the LHC to provide more discrimination among theoretical models.

[Learn more](#)

—edited by Dino Goulianos and Andy Beretvas

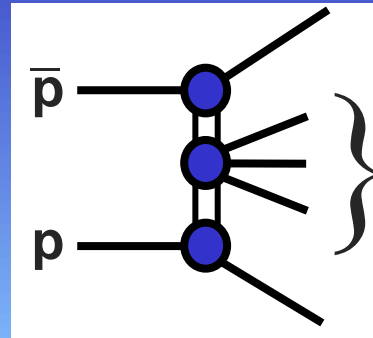
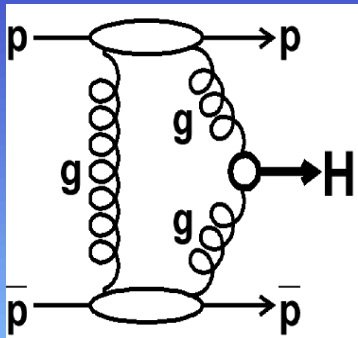


A scintillator fiber tracker (RPS) is used to observe diffractive events as a function of the momentum transfer between the incoming and outgoing antiproton.

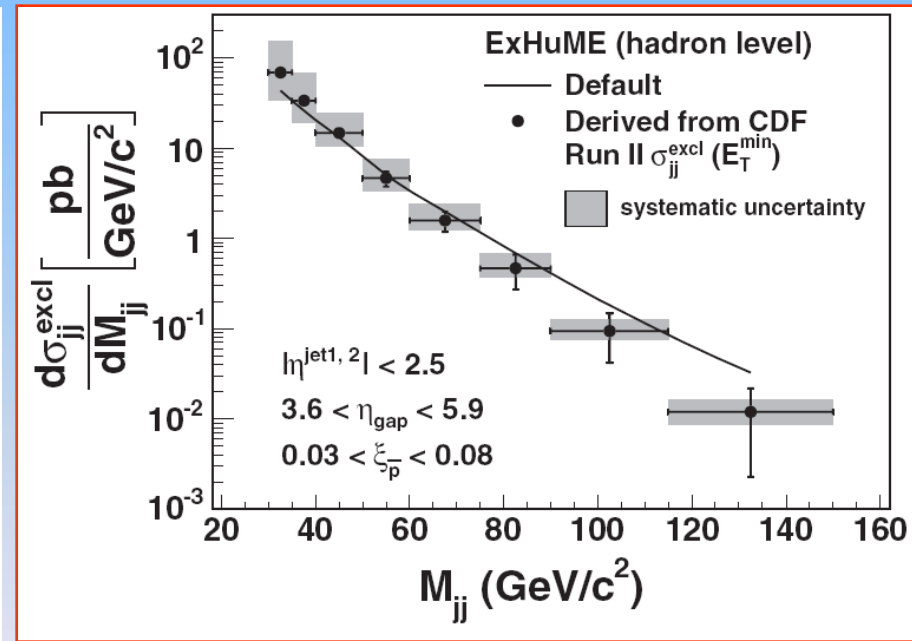
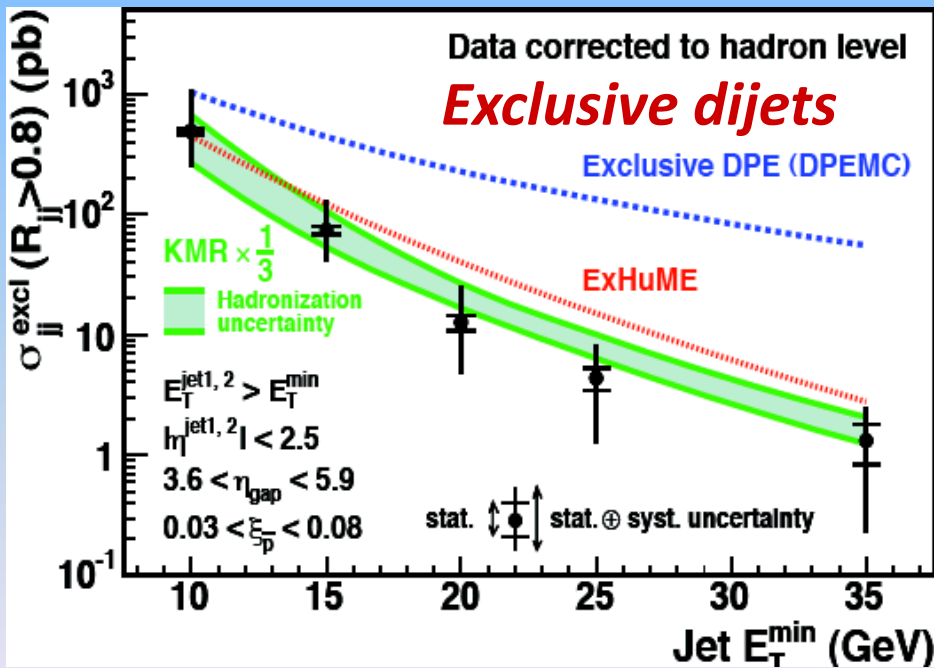


These physicists were responsible for this analysis. From left: Michele Gallinaro, Dino Goulianos and Koji Terashi, all from Rockefeller University.

EXCLUSIVE Dijet \rightarrow Excl. Higgs THEORY CALIBRATION



PRD 77, 052004 (2008)



CDF @ LHC

- ❑ Larger Energy → Larger ET
- **Multigap** diffraction
- **Diffraction Higgs** production

- ❑ The CDF measurements are having an impact on all LHC physics
→ the **MBR (Minimum Bias Rockefeller) simulation is now in PYTHIA8**

arXiv.org > hep-ph > arXiv:1205.1446

High Energy Physics - Phenomenology

MBR Monte Carlo Simulation in PYTHIA8

R. Ciesielski, K. Goulianos

(Submitted on 7 May 2012)

Summary

- We measured SD to ND ratios in dijet production vs Bjorken- x for $\langle Q^2 \rangle$ up to 10^4 GeV^2 and $-t > 4 \text{ GeV}^2$
- We find:
 - ✓ nearly identical E_T^{jet} distributions for SD and ND events
 - ✓ small $\langle Q^2 \rangle$ dependence as a function of Bjorken- x
 - ✓ no $\langle Q^2 \rangle$ dependence of the b-slopes at low t
 - ✓ t distributions compatible with DL at low t
 - ✓ at high t the distributions lie increasingly higher than DL, becoming approximately flat for $-t > 2 \text{ GeV}^2$
 - compatible with a diffraction minimum at $-t > 2.5 \text{ GeV}^2$
- Our findings are compatible with models of diffraction in which the hard scattering is controlled by the PDF of the recoil antiproton, while the rapidity gap formation is governed by the color-neutral soft exchange.

Thank you for your attention

BACKUP

Data samples

TABLE I. The number of events surviving successive selection requirements by data sample.

Selection requirement	RPS	RPS · Jet5	RPS · Jet20	RPS · Jet50
Trigger level	1 634 723	1 124 243	1 693 644	757 731
Good-run events	1 431 460	955 006	1 421 350	561 878
\cancel{E}_T significance: $S_{\cancel{E}_T} \equiv \cancel{E}_T / \sqrt{\sum E_T^2} < 2$	1 431 253	950 776	1 410 780	539 957
$N(\text{jet}) \geq 2: E_T^{1,2} > 5 \text{ GeV}, \eta^{1,2} < 2.5$	59 157	557 615	1 168 881	521 645
Splash veto	27 686	259 186	541 031	215 975
RPT	27 680	259 169	541 003	215 974
SD ($0.03 < \xi_{\bar{p}}^{\text{CAL}} < 0.09$)	1 458	20 602	26 559	4 432

TABLE II. Data sets of MB events collected with a $\text{CLC}_{\bar{p}} \cdot \text{CLC}_p$ coincidence requirement at various periods during the data-taking run, corresponding integrated luminosities, L , and triple-coincidence RPT counter efficiencies, ϵ_{RPT} .

Data set	L (pb^{-1})	ϵ_{RPT}
set 0	12.9	0.78 ± 0.08
set 1	24.0	0.75 ± 0.08
set 2	20.3	0.69 ± 0.07
set 3	6.4	0.57 ± 0.06
set 4	29.2	0.51 ± 0.05
set 5	16.3	0.46 ± 0.05
set 6	18.9	0.48 ± 0.05
set 7	25.5	0.43 ± 0.04
set 8	22.1	0.40 ± 0.04

Ratio of SD to ND events vs E_T^*

Source of uncertainty	Variation	$\Delta \mathcal{R}_0$	Δr
Underlying event	$\pm 30\%$	$\pm 3\%$	$\mp 5\%$
Central/plug cal. energy scale	$\pm 5\%$	$\pm 8\%$	$\sim 3\%$
MiniPlug energy scale	$\pm 30\%$	$\mp 6\%$	$\pm 1\%$
Tower E_T threshold	$\pm 10\%$	$\pm 1\%$	$\pm 1\%$
Overlaps in ND events	$\pm 20\%$	$\pm 8\%$	$< \pm 1\%$
Instantaneous luminosity	$\pm 6\%$	$\pm 3\%$	N/A
Bunch-by-bunch luminosity	$\pm 50\%$	$\pm 4\%$	N/A
RPS acceptance	N/A	$\pm 10\%$	N/A
Splash events	N/A	$\pm 6\%$	N/A
Total uncertainty		$\pm 18\%$	$\pm 6\%$

TABLE III

$$\mathcal{R} = \mathcal{R}_0 \cdot (x_{Bj}/0.0065)^r$$

TABLE IV. Fit parameters of the ratio of SD to ND production rates for events in different E_T^* bins. The ratios are fitted to the form $\mathcal{R} = \mathcal{R}_0 \cdot x_{Bj}^r$ for $1 \times 10^{-3} < x_{Bj} < 2.5 \times 10^{-2}$.

Jet E_T^* [GeV]	Q^2 GeV ²	\mathcal{R}_0	r
$8 < E_T^* < 12$	100	$(8.6 \pm 0.8) \times 10^{-3}$	-0.44 ± 0.04
$18 < E_T^* < 25$	400	$(8.0 \pm 1.6) \times 10^{-3}$	-0.48 ± 0.05
$35 < E_T^* < 50$	1600	$(6.3 \pm 1.8) \times 10^{-3}$	-0.60 ± 0.07
$50 < E_T^* < 70$	3000	$(5.5 \pm 5.0) \times 10^{-3}$	-0.64 ± 0.22
$70 < E_T^* < 90$	6000	$(7.0 \pm 7.0) \times 10^{-3}$	-0.58 ± 0.26

Slopes of t -distributions

TABLE V. Slopes of t distributions for soft and hard diffractive events of the SD RPS_{track} data in the range $0.05 < \xi_p^{\text{RPS}} < 0.08$ for different $\langle E_T^* \rangle$ or $Q^2 \equiv \langle E_T^* \rangle^2$ bins obtained from fits to the form of Eq. (7), $d\sigma/dt = N \cdot (A_1 \cdot e^{b_1 \cdot t} + A_2 \cdot e^{b_2 \cdot t})$, with $A_2/A_1 = 0.11$, fixed at the average value obtained in the dynamic alignment of all different event subsamples. The uncertainties listed are statistical.

Event sample (definition)	$\langle E_T^* \rangle$ (GeV)	Q^2 (GeV ²)	b_1 (GeV ⁻²)	b_2 (GeV ⁻²)	b_1/b_1^{incl} (ratio)	b_2/b_2^{incl} (ratio)
RPS	incl	≈ 1	5.4 ± 0.1	1.2 ± 0.1	1	1
RPS · Jet5	15	225	5.0 ± 0.3	1.4 ± 0.2	0.93 ± 0.08	1.12 ± 0.23
RPS · Jet20	30	900	5.2 ± 0.3	1.1 ± 0.1	0.96 ± 0.07	0.93 ± 0.16
RPS · Jet50	67	4500	5.5 ± 0.5	0.9 ± 0.2	1.00 ± 0.10	0.72 ± 0.18

TABLE VI. Systematic uncertainties in the slope parameters b_1 and b_2 of the diffractive t -distributions (from Table V).

Source of uncertainty	δb_1	δb_2
RPS tracker threshold	1%	1%
Instantaneous luminosity	2%	2%
Beam conditions	4%	8%
RPS alignment	5%	5%
Total (quadrature-sum)	6.8%	9.7%

RIGGERS AND EVENT SAMPLES

- RPS_{track} : RPS with RPS tracking available (included in the RPS trigger);
- J5, J20, J50: jet with $E_T^{\text{jet}} \geq 5, 20, 50$ GeV in CCAL or PCAL;
- RPS·Jet5 (Jet20, Jet50): RPS in coincide with J5, J20, J50.

Event sample	$\langle E_T^* \rangle$ GeV	Q^2 GeV ²
RPS	incl	≈ 1
RPS·Jet5	15	225
RPS·Jet20	30	900
RPS·Jet50	67	4500

The end!